DR. STACEY BEDWELL (Orcid ID : 0000-0003-3283-7748)



Article type : Research Report

# Mapping of Fine Scale Rat Prefrontal Cortex Connections: Evidence for Detailed Ordering of Inputs and Outputs Connecting the Temporal Cortex and Sensory-Motor Regions

Authors: Stacey A Bedwell[1], and Chris J Tinsley[2]

Corresponding author:

Stacey Bedwell

stacey.bedwell@bcu.ac.uk

[1]Department of Psychology

Birmingham City University

Cardigan St.

Birmingham

B4 7BD

[2]School of Science and Technology

Nottingham Trent University

Clifton Lane

Nottingham

NG11 8NS

This article has been accepted for publication and undergone full peer review but has not been through the copyediting, typesetting, pagination and proofreading process, which may lead to differences between this version and the Version of Record. Please cite this article as doi: 10.1111/ejn.14068

Running title: Mapping of Fine Scale Rat Prefrontal Cortex Connections

Keywords

Prefrontal Cortex, ordering, connections, temporal cortex, rat.

Acknowledgements

This work was supported by a Nottingham Trent University studentship awarded to Stacey Bedwell. We would like to acknowledge the technical assistance from Andrew Marr.

Conflicts of Interest

The authors declare no conflict of interests.

Data Statement

On acceptance of this article we plan to deposit the connectional data on the University of Rostock rat connectome website: http://neuroviisas.med.uni-rostock.de/connectome/index.php. The Data File(s) will also be deposited to Figshare.

Author contributions

S.A. Bedwell – Literature review, study design, data collection, data analysis and interpretation, manuscript writing.

C.J. Tinsley – study design, data collection, manuscript writing.

**Abstract**

Cerebral cortex structure is crucially important for cortical organisation and function. The organisation of prefrontal cortex (PFC) is controversial and here we seek to understand it more clearly through the study of fine scale cortical connections. To determine the ordering of micro-scale input and output connections in the rat PFC we injected small volumes (20-30nl) of anterograde (Fluro-

Ruby) and retrograde (Fluoro-Gold) neuroanatomical tracers into PFC. These injections revealed several connected regions of the brain but here we report findings restricted to PFC to temporal cortex and sensory-motor cortex pathways. In agreement with previous studies incorporating larger injection volumes we found that smaller injection volumes revealed a more detailed, fine scale ordering of both prefrontal inputs and output connections to the temporal cortex and sensory-motor cortex regions. These findings are also supported by labelling observed from additional tracer injections made into corresponding regions of temporal cortex. The topography observed reflected the ordering seen at a larger level (i.e with larger injection volumes) but there were some differences in the topography, such as in relation to the direction of ordering. In agreement with earlier work, we found that fine scale input and output connections were not always aligned with respect to one another. These results provide evidence for topographically arranged inputs and outputs in two distinct PFC pathways, along with evidence for different connectional patterns within the same pathways. Based on theories of functional connectivity, these findings provide evidence for prefrontal cortical regions residing within networks that contribute to different cognitive functions.

## Introduction

The parallel arrangement of input and output projections, and therefore reciprocal connections, is a widely accepted property of cortical organisation. Such parallel arrangement of connections has been described in perirhinal, postrhinal, entorhinal, piriform, frontal, insular, temporal, cingulate, parietal and occipital cortices (Canto et al, 2008; Agster & Burwell, 2009). Physiological studies have reported mapping of delayed spatial responses in the principal sulcus region of primates (Sawaguci & Iba, 2001). Imaging studies have also reported mnemonic mapping of responses in human dorsolateral prefrontal cortex (Hagler & Sereno, 2006). Elsewhere, in ferret visual cortex, topographically organised connections support physiological maps and there is evidence that the input and output connections are reciprocal (Cantone et al, 2005). Pathways such as LGN to V1 (Perkel et al, 1986) and V2 to V1 (Sousa et al, 1991) in monkeys are reported to display topographically organised

connections. Topographically ordered and reciprocal connections have been reported in pathways between visual cortex and areas of sensory-motor cortex in rats (Miller and Vogt, 1984). The same study suggested that ordered reciprocal connections in the visual cortex provide a means for integration of information, thus implying that reciprocal, ordered connectivity is an important basis for complex processing. Notably, the same paper also reported large numbers of non-reciprocal connections between perirhinal and visual cortex, indicating that complex cortical networks are not always entirely reciprocal.

In prefrontal cortex there is evidence for ordered connections as that seen in other complex regions e.g. visual cortex (Sesack et al, 1989; Vertes, 2004; Hoover & Vertes, 2011; Bedwell et al, 2014, 2015 & 2017; Kondo & Witter, 2014; Delatour & Witter, 2002; Reep 1996). Ordered connectivity (i.e. topography or topology) has been reported in the pathways linking rat prefrontal cortex to subcortical regions (Berendse et al, 1992; Sesack et al, 1989) and other cortical regions, notably temporal cortex (Hoover & Vertes, 2011; Kondo & witter, 2014; Bedwell et al, 2015 & 2017) as well as sensory-motor cortex (Bedwell et al, 2014 & 2017). Anterograde tracing studies in rats have identified reciprocal topographic connections from perirhinal, postrhinal and ectorhinal regions (Agster & Burwell, 2009), although the degree of reciprocity was reported to vary greatly between these regions. Topological subcortical connections from PFC have also been observed in the PFC – striatum pathway (Berendse et al., 1992; Schilman et al., 2008).

In the rat medial PFC (mPFC) and orbital PFC (OFC) are understood to be functionally distinct (Schoenbaum and Roesch, 2005; Schoenbaum and Esber, 2010). Medial PFC is known to play important roles in the timing of motor behaviours (Narayanan and Laubach, 2006; Narayanan and Laubach, 2008; Narayanan and Laubach, 2009; Smith et al., 2010; Kim et al., 2013) and orbital PFC is involved in processing expected outcomes of events (Schoenbaum and Esber, 2010; Schoenbaum and Roesch, 2005; Stalnaker et al., 2015). Consistent with these different functional associations, our

previous findings have shown evidence for differences in connectional organisation between mPFC and OFC in rats (Bedwell et al, 2014, 2015, 2017).

Typically, the topological ordering of PFC connections has been described along the medial lateral axis. Changes in the organisation of rat cingulate PFC connections along the anterior-posterior (A-P) axis have also been identified (Olson and Musil, 1992). It is unclear whether or not this is a wider organisational principle also present in other regions, or what the precise functional relevance of such an organisation might be. However, it has been proposed that there are changes in cognitive processing characteristics, such as abstraction in anterior compared to posterior prefrontal cortex in humans (Taren et al., 2011). Such changes in cognitive processing are supported by evidence of an anterior to posterior reciprocity gradient in terms of anatomical connectivity (Bedwell et al, 2017).

In previous studies we found evidence for broadly ordered and unaligned input and output connections in the pathway linking rat prefrontal (prelimbic [PL], medial orbital [MO], ventral orbital [VO], ventral lateral orbital [VLO], lateral orbital [LO], dorsal lateral orbital [DLO]) and temporal (perirhinal [Prh], entorhinal [Ent]) cortex (Bedwell et al, 2015 & 2017), as well as the pathway linking prefrontal (PL, MO, VO, VLO, LO, DLO) and sensory-motor (primary motor [M1], secondary motor [M2], primary somatosensory, jaw region [S1J], primary auditory [Au1]) cortex (Bedwell et al, 2014 & 2017). Our findings consistently show input and output connections from PFC producing labelling in different regions of temporal and sensory-motor cortex. For instance, tracer injections made into VO consistently produce anterograde and retrograde labelling in distinctly different temporal regions (anterior – posterior).

Reports describe topographically organised connections from temporal (Delatour and Witter, 2002; Arnault and Roger, 1990; Burwell et al., 1995) and sensory-motor (Porter and White, 1983; Aronoff et al., 2010; Henry and Catania, 2006) cortex to regions other than PFC in rats. Taken with our observations of ordered topological connectivity, logically, this points towards topographically ordered connections in the PFC–temporal and PFC–sensory-motor pathways. Evidence for topographically ordered PFC connections has been shown in previous studies (Bedwell et al, 2014, 2015, 2017). Previous reports also indicate a complex relationship between input and output connections in these pathways.

Although we have established a differential organisational structure in PFC pathways in comparison with other cortical regions, it remains unclear exactly how the precise circuitry of PFC is organised. In order to clearly establish the nature of physiological organisation within PFC, it is necessary to first gain a more detailed picture of the underlying anatomical connectivity. Conde et al (1995) described ordered connections from small regions within medial PFC to areas of temporal cortex. This type of high resolution study allows multiple injection sites to be placed within a single cytoarchitectural region, enabling a description of ordering which is overlooked on a larger scale i.e. between sub-regions within a cytoarchitectural region. The use of small tracer injection volumes by Conde et al (1995) provided a valuable insight into the anatomical microcircuitry between regions of medial PFC and temporal cortex. In applying the same principle to the investigation of prefrontal cortex connections across several regions, we aimed to reveal the smaller organisational properties underlying the largescale arrangement already identified.

Prefrontal cortex is defined as the projection target of the mediodorsal nucleus of the thalamus (Rose & Woolsey, 1948). More recent findings have expanded this definition to PFC having stronger connections with the mediodorsal thalamic nucleus than other nuclei of the thalamus (Uylings et al, 2003); this is a definition which remains in use in the recognition of PFC across mammalian species

and is employed in this study. For the purpose of anatomical investigations, here we define PFC sub-regions according to Van de Werd & Uylings (2008).

In this study we sought to address whether our previously observed unique relationships between afferent and efferent projections could be seen at a finer scale and in the same pathways (PFC – temporal cortex and PFC – sensory motor cortex) as those described on a broader scale thus providing a more detailed microscopic understanding of prefrontal cortex structure. By employing a higher resolution analysis, utilizing smaller tracer injection volumes placed closer together, we were able to provide a better level of resolution for observing connectional patterns that are possibly obscured by larger volume injections. We were able to reveal the smaller scale organisational properties underlying the largescale arrangement already identified (Bedwell et al 2014, 2015, 2017). This higher resolution analysis enabled us to establish that there is a detailed topographic ordering of both input and output connections at a level of detail and precision which has not previously been described. This was the case for connections to both temporal and sensory motor cortices. In addition we established that the pattern of topographic PFC afferents and efferents showed varied levels of reciprocity in both pathways.

## Methodology

### *Animals*

#### *Ethical Statement*

All Animal procedures were carried out in accordance with the UK Animals scientific procedures act (1986), EU directive 2010/63 and were approved by the Nottingham Trent University Animal Welfare and Ethical Review Body.

*Experimental Animals*

Seventeen male CD rats (table 1) were obtained from Charles River, UK. On receipt the animals were examined for signs of ill-health or injury. The animals were acclimatized for ten days during which time their health status was assessed. At the start of the surgery the animals' weight range was 314g to 358g.

Prior to surgery the animals were housed together in individually ventilated cages (IVC) (Techniplast double decker Greenline rat cages). The animals were allowed free access to food and water. Mains drinking water was supplied from polycarbonate bottles attached to the cage. The diet and drinking water were considered not to contain any contaminant at a level that might have affected the purpose or integrity of the study. Bedding was supplied by IPS Product Supplies Ltd in form of 8/10 corncob. Environmental enrichment was provided in the form of wooden chew blocks and cardboard fun tunnels (Datesand Ltd., Cheshire, UK). Post-surgery the animals were individually housed in the same conditions. The animals were housed in a single air-conditioned room within a barrier unit. The rate of air exchange was at least fifteen air changes per hour and the low intensity fluorescent lighting was controlled to give twelve hours continuous light and twelve hours darkness. The temperature and relative humidity controls were set to achieve target values of 21 ± 2ºC and 55 ± 15% respectively.

*In vivo observations*

Individual bodyweights were recorded on Day -10 (prior to the start of dosing) and daily thereafter. All animals were examined for overt signs of ill-health or behavioural change immediately prior to surgery dosing, during surgery and the period following surgery. There were no observed clinical signs/ symptoms of toxicity or infection. There was no significant effect on body weight development detected.

*Surgical and Experimental Procedures*

Rats were anesthetised with isoflurane (Merial, Harlow, UK) at a flow rate of 2l/min 93 % oxygen and at an average concentration of 2.5% isoflurane (using an Oxy Vet Oxygen concentrator (Eickemeyer, UK) and a Fortec Isoflurane vaporizer). Analgesia in the form of Buprenorphine (0.05mg/kg i.m/s.c) and Meloxicam (up to 1mg/kg s.c/orally) were administered peri-operatively and for several days post-operatively. Rats were placed in a stereotaxic frame and the incisor bar set to achieve a flat skull. Body temperature was monitored during and immediately after surgery using a rectal thermometer. Craniotomies (< 1mm diameter) were made at predetermined stereotaxic coordinates. Sterile tracer solution was deposited into the prefrontal and temporal cortices via a 0.5µl Neuro-syringe (Hamilton, Germany). Injections of anterograde (10% Fluoro-ruby in distilled water, Fluorochrome, Denver, Colorado), retrograde tracer (4% Fluoro-Gold in distilled water, Fluorochrome, Denver, Colorado) were made into the prelimbic (PL), infralimbic (IL), medial orbital (MO), ventral orbital (VO), ventrolateral orbital (VLO), lateral orbital (LO) or dorsolateral orbital cortex (DLO), with the intention of revealing the fine scale anatomical connections of prefrontal regions. The distance between craniotomy co-ordinates (0.5mm) was based on the measured spread of tracers in preliminary and the present studies (<0.5mm in diameter).

Each rat received injections of Fluoro-gold (30nl, 100nl/min) and Fluororuby (20nl, 10nl/min) into various subdivisions of PFC (+4.2mm anterior to bregma, according to Paxinos & Watson, 1998), separated by 1mm (fig. 1) or Fluoro-Gold (50nl, 100nl/min) and Fluorescein (50nl, 100nl/min) into regions of temporal cortex (-2.8mm to -4.8mm posterior to bregma, according to Paxinos & Watson, 1998), separated by 0.5mm (fig. 9). Fluoro-Gold was injected into one side of the brain and Fluro-Ruby was injected into the other side for PFC injection studies. In temporal cortex injection studies dual injections of Fluoro-Gold and Fluorescein (biotinylated dextran amine (BDA); Fluorescein ([SP-1130] Vector Laboratories, CA) were made into the same sites. Projections were observed to be confined to the ipsilateral hemisphere of the brain. Additional and equivalent Fluoro-Gold injections

were made into the left and right hemispheres in previous studies (Bedwell et al, 2014) to verify whether the location and ordering of projections differed on the either side of the brain. The same overall order and positioning of Fluoro-Gold labelling was observed on both sides of the brain.

Following a survival time of 7-8 days, the rats were deeply anesthetized using pentobarbital (Sigma-Aldrich, UK), and transcardially perfused with 0.1M phosphate buffered saline (PBS) (~200ml) followed by 4% paraformaldehyde (PFA) (~200ml) in PBS. The brain was removed and stored for 24 hours in 4% PFA in 0.1M PBS, followed by cryoprotection in 30% sucrose in 0.1M PBS.

### *Anatomical processing and Microscopic Analysis*

#### *Anatomical processing*

For analysis of anterograde and retrograde connections, two series of 40μm coronal sections were taken (2 in 6 sections) on a freezing microtome (CM 1900, Leica, Germany) and mounted onto gelatin coated slides. Sections were cover slipped with Vectashield® mounting medium (with propidium iodide) for fluorescent imaging of Fluoro-Gold or Vectashield® mounting medium (with DAPI) for fluorescent imaging of Fluoro-Ruby labelled axon terminals. Fluorescent photos were captured using an Olympus DP-11 system microscope with a x4 and x10 objective lens.

#### *Microscopic Analysis*

The entire forebrain was examined for labelling. Based on previous findings of PFC broad scale connections, temporal and sensory-motor regions were examined for retrograde and anterograde labelling. A detailed analysis was carried out on these regions to determine the underlying fine scale organisation of PFC – temporal and PFC- sensory-motor cortex connections.

The use of Fluoro-Ruby as an anterograde tracer in comparison to BDA used in our previous studies (Bedwell et al 2014, 2015 & 2017) allowed for a more precise measuring of anterograde labelling, in which the 3-dimensional location of labelled axon terminals could be recorded, in the same manner as Fluoro-Gold labels.

ImageJ (Wayne Rasband, NIH) was used to determine numerical values representing the location of retrograde and anterograde labels in temporal cortex. The three dimensional location of each labelled cell or axon terminal was calculated by measuring the distance from (in temporal cortex) the rhinal sulcus (Dorsal-ventral and Medial-lateral), the anterior-posterior location of each labelled cell/axon terminal was recorded in terms of distance from Bregma (according to Paxinos and Watson, 1998). In sensory-motor cortex and prefrontal cortex labels were measured in terms of distance from dorsal cortical surface (dorsal-ventral), medial cortical surface (medial-lateral) and distance from Bregma (anterior-posterior).

## Results

We sought to establish the order and organisation of fine scale input and output connections to rat prefrontal cortex. We studied the organisation of input and output connections to prefrontal cortex using the retrograde tracer, Fluoro-Gold and the anterograde tracer, Fluoro-Ruby. Both anterograde and retrograde connections to prefrontal cortex were visualised in temporal cortex and sensory-motor cortex, resultant from equally spaced PFC injections into PL, IL, MO, VO, VLO, LO and DLO (according to Van De Werd & Uylings, 2008). Additional anterograde and retrograde labelling in PFC resultant from dual tracer injections (Fluoro-Gold and Fluorescein) was analysed. Here we report the results of an in-depth analysis into the location of both anterograde and retrograde connections from PFC to temporal and sensory-motor cortices.

*Organisation of input and output connections from PFC to temporal cortex*

Fluoro-Gold (30nl) injection sites were positioned in the intended PFC regions (fig. 1). Retrograde injection sites spanned layers II –VI. There was some minimal overlap between injections made into PL, IL, MO and VO (A&B, B&C and B&D). There was also a small overlap of the spread of tracer at injection sites into LO and DLO (F&G). The majority of the spread of tracer at retrograde injection sites was confined to the intended cytoarchitectural region and the seven injection sites were evenly spaced from one another.

Fluoro-Ruby injection sites were found in the intended regions of PFC (fig. 1). The spread of Fluoro-Ruby at 20nl injection sites was comparably smaller than the equivalent 30nl Fluoro-Gold injection sites, due to the smaller injection volume as well as the consistent smaller spread of Fluoro-Ruby. Fluoro-Ruby injection sites were predominantly confined to the intended cytoarchitectural regions of PFC and were found to be mostly within the borders of the equivalenet 30nl Fluoro-Gold injection sites. There was some overlap between injection sites into LO and DLO (F [LO/DLO] & G [DLO]). The Fluoro-Ruby injection sites spanned layers III-VI and were found to be equally spaced from one another.

Projections to PFC from temporal cortex were seen in perirhinal (PRh), Ectorhinal (Ect), lateral entorhinal cortex (LEnt) and secondary auditory cortex, ventral area (AuV) (fig. 2). The distribution of retrogradely labelled cells within temporal cortex maintains a spatial order in accordance with the corresponding Fluoro-gold injection sites in PFC (fig. 3 & 4). The most prominent ordering can be seen in the anterior-posterior axis. Moving from medial to lateral in terms of PFC injection sites, retrograde labelling in temporal cortex moves from anterior to posterior (injection sites B [PL] – G [DLO]).

Projections from PFC to temporal cortex were seen in PRh, Ect, temporal association cortex (TeA), AuV and LEnt (fig. 2). The distribution of anterogradely labelled cells within temporal cortex also maintains an overall spatial order in accordance with their corresponding Fluoro-ruby injection sites in PFC (fig. 3 & 4). The most prominent ordering can be seen in the dorsal-ventral axis. Moving from medial to lateral in PFC, anterograde labels in temporal cortex move from ventral to dorsal (injection sites A [PL/M2] – D [VO/VLO]). Fluoro-ruby is seen in the same cytoarchitectural regions as its BDA counterpart from, reported in previous studies (Bedwell et al. 2015), however is more clearly visualised and can be seen spread over a larger area. A level of convergence remains; as anterogradely labelled cells appear in a smaller area than retrogradely labelled cells from the same PFC injection sites. A clear three dimensional representation of labelling in temporal cortex can be seen in figure 8 (i & ii).

*Organisation of fine scale input and output connections from prefrontal cortex to sensory-motor cortex*

Projections to PFC from regions of sensory-motor cortex were seen in cingulate cortex (Cg1, Cg2), motor cortex (M2, M1), somatosensory cortex (S1J, S1JO, S1BF) and piriform cortex (pir) (fig. 5). The distribution of retrogradely labelled cells within sensory-motor cortex maintains a spatial order in accordance with the corresponding Fluoro-Gold injection sites in PFC (fig.6 & 7). The clearest ordering can be seen in the dorsal-ventral axis, moving from medial to lateral in PFC, retrograde labels in sensory-motor cortex move from dorsal to ventral (injection sites A – D) and then from ventral to dorsal (injection sites D – G).

Projections from PFC to sensory-motor cortex were seen in Cg1, Cg2 and M2 (fig. 5). The distribution of anterogradely labelled cells within sensory-motor cortex maintains a spatial order in accordance with the corresponding Fluoro-Ruby injection sites in PFC (fig.6 & 7). Fluoro-Ruby is

seen in the same cytoarchitectural regions as its BDA counterpart from, reported in previous studies (Bedwell et al. 2014), however it is more clearly visualised and can be seen spread over a larger area. A level of convergence remains; as anterogradely labelled cells appear in a smaller area than retrogradely labelled cells from the same PFC injection sites. A clear three dimensional representation of labelling in sensory motor cortex can be seen in figure 8 (iii & iv).

*Organisation of fine scale connections in comparison to broad scale connections*

A direct comparison of broad (from large volume injections, separated by 1mm) and fine scale (from small volume injections separated by 0.5mm) connectivity patterns, using a comparison of Euclidean distances between corresponding retrograde and anterograde labels from equivalent PFC injection sites indicated similar overall ordering in regards to the relationship between input and output connections. This means that the overarching broad scale pattern is evident and was replicated in our smaller scale findings.

A comparison of retrograde and anterograde labelling found in sensory-motor cortex from 20-30nl tracer injections vs. 100nl tracer injections (Bedwell et al, 2014) revealed no observable differences in the midpoint location of retrogradely labelled cells in sensory-motor cortex between 30nl and 100nl Fluoro-Gold injections (in the dorsal-ventral axis the anterior-posterior axis and the medial-lateral axis. No differences in the midpoint location of anterograde labelling in sensory-motor cortex between 20nl and 100nl Fluoro-ruby injections (in the dorsal ventral axis, in the anterior-posterior axis and the medial-lateral axis) was found. This shows that the overall organisational pattern of PFC-sensory-motor cortex connections seen from these fine scale tracer injections is consistent with that seen on a broader scale, for both input and output connections.

In order to ensure that labelling from the BDA used in earlier studies (Bedwell et al, 2014) and Fluoro-Ruby used in the present were comparable, a comparison of labelling was made of 100nl anterograde BDA injections with 100nl anterograde Fluoro-Ruby injections. No difference was found between 100nl sensory-motor cortex labelling with BDA and Fluoro-Ruby. Therefore resultant labelling from the two different anterograde tracers is comparable.

*Comparison with ordering resultant from injections into temporal cortex*

A series of 50nl injections of Fluoro-Gold and Fluorescein (fig. 9) were made into five sites in temporal cortex, corresponding to the temporal areas labelled by PFC tracer injections in the present and earlier studies. Tracer injections were made at equally spaced locations along the anterior-posterior axis (Bregma -2.8, -3.3, -3.8, -4.3, -4.8 mm). We revealed a similar pattern of connectivity in labelling in PFC resultant from tracer injections made into temporal cortex as that seen in temporal regions resultant from PFC injections. Moving from anterior – posterior in temporal cortex revealed ordered labelling (for both Fluoro-Gold and BDA) along the medial-lateral and dorsal-ventral axes in PFC (fig. 10 & 11).

There are some minor discrepancies, in that labels in PFC are not confined to the specific cyoarchitectural regions and do not mirror labelling seen in temporal cortex exactly, however the overall ordering is comparable to that described from PFC tracer injections and differences are likely to be due to differences in injection site vs. labelled regions in temporal cortex. These findings provide further support for the observed ordering of connections.

*Connectional Architecture of prefrontal cortex*

*Temporal cortex*

Having outlined the evidence for ordered prefrontal input and output connections the question remains as to what the organisational architecture of prefrontal cortex is. We used the present data from PFC (20-30nl) tracer injections to produce a connectivity matrix where the locations of retrograde and anterograde labels were plotted with respect to injection sites. For a given area within temporal cortex containing the retrograde label, we assessed which injection sites produced anterograde labelling in the same area (Fig. 12). From the matrix we can see that for each temporal cortex site (PFC input site) there is a considerable return projection from other prefrontal cortex sites (which are often not neighboring sites within prefrontal cortex). There is one retrograde labelled site within temporal cortex (PFC afferent site), F (LO/DLO), which contains a feedback projection from the majority of the other prefrontal cortex sites (by comparison perfectly reciprocal input and output connections would produce an alignment with a diagonal band).

A further investigation of the relationship between input and output connections in this pathway revealed that when examining retrograde and anterograde labels found in the same cytoarchitectural region of temporal cortex, the median distance between source injection sites decreases from medial to lateral (PL to VLO). This change in connectivity between regions is demonstrated by figure 13. Retrograde and anterograde connections are found closest together in the temporal cortex region receiving the VLO retrograde projection. It is worth noting that although PL has the most widespread connections and shows a considerable amount of non-reciprocal labelling (as shown by figures 12 and 13). A high degree of reciprocity in PL can also be easily seen by a simplified reciprocity index, calculated from the minimum distance between retrograde and anterograde PFC injection sites within the connectivity matrix entries in figure 12. Within temporal cortex and for PL, this distance is 0 (indicating high reciprocity), whereas for other regions (IL/MO/VO/VLO) it is 1 (indicating lower reciprocity). For VLO/LO/DLO this distance = 0. Taken together for temporal cortex, we can see that

small regions of cortex send and receive some highly reciprocal PFC connections but also non-reciprocal PFC connections. This indicates a clear non-parallel organization for this important brain circuit.

*Sensory-motor cortex*

A similar connectivity matrix was constructed from the fine scale connections between prefrontal and sensory-motor cortex (Fig. 14). As with temporal cortex, this matrix shows evidence of widespread feedback projections, from widespread PFC regions and relatively little reciprocity. Injection site B (PL) is the only location to show evidence of complete reciprocity. It is evident from figure 14that specific areas of PFC receive feedback from very widespread regions of PFC in this PFC-sensory-motor cortex circuit, whereas others receive feedback from a more limited region. A simple calculation of the minimum distance between retrograde and anterograde PFC injection site clearly demonstrates this difference, PL (injection site B) is the only region with a distance of 0, in DLO this value is as great as 5.

A further investigation of the relationship between input and output connections in this pathway revealed that when examining retrograde and anterograde labels found in the same cytoarchitectural region of sensory-motor cortex, the median distance between source injection sites increases from medial to lateral (VO to DLO). This change in connectivity between regions is demonstrated by figure 15.

## Discussion

The results presented here provide evidence that when visualised on a fine scale, rat prefrontal cortex receives inputs and sends outputs from temporal cortex and sensory-motor cortex that have a detailed and topographic order. The findings also show that there are differences in reciprocity between

afferents and efferents visualised by injecting anterograde or retrograde tracers into equivalent PFC sites.

*Comparison to previous studies of prefrontal connectivity*

Previous studies of rat prefrontal cortex connections have reported connections with the temporal cortex (Sesack, 1989; Hoover & Vertes, 2011). There have also been reports of an ordered arrangement of output connections from PFC: moving from medial to lateral (in terms of injection site) previous studies showed signs of an arrangement of PFC output connections in the dorsal-ventral axis of temporal cortex (Hoover & Vertes, 2011) and a detailed and topographically organized PFC output projection to temporal cortex (Kondo & Witter, 2014). There have also been reports of ordered connections between primate prefrontal cortex and the medio-dorsal nucleus of the thalamus (Giguere et al, 1988) and the parietal cortex (Cavada et al, 1989a, 1989b) . Therefore the present results are in agreement with these previous reports outlining an ordering of prefrontal connections, but also highlight a more complex underlying anatomical organisation of prefrontal cortex connections.

Primate studies have identified multiple anatomical networks within PFC, associated with distinct functions (Ongur & Price, 2000; Saleem et al, 2014). The findings presented here show consistent evidence of distinct, parallel PFC networks within the rat PFC. Our findings have additionally revealed evidence for differential organisation and structural properties within overlapping PFC networks. The results presented here provide evidence to support Bayer & Altman's (1991) findings of different neurogenetic patterns of development within the endopiriform nucleus and claustrum, implying that different patterns of connectivity identified here are the result of different developmental patterns.

*Comparison to analogous experiments of broader scale prefrontal-temporal connections*

A previous study (Bedwell et al, 2015) utilized the same part of the prefrontal-temporal cortex pathway but used larger volumes of tracer (100nl) and a different anterograde tracer (i.e. biotinylated dextran amine as opposed to Fluoro-Ruby). Comparisons of 100nl vs. 20-30nl data showed similar patterns in overall organisation of connections. A comparison of broad and fine scale connectivity patterns, using a comparison of Euclidean distances between corresponding retrogradely and anterogradely labelled cells, indicated similar patterns of organization with regards to the relationship between input and output connections; these analyses indicated no significant differences between the overall organisational pattern at 100nl and 20-30nl. The ordering was similar for both broad and fine scale analysis of the prefrontal-temporal pathway (i.e. the order was of an equivalent direction and magnitude across the cortical surface). However, the apparent order seen at a broad scale was more complex when viewed at a finer scale. For example, the direction of ordering appeared to be reversed across certain injection sites when viewed on a broad scale. However, when viewed on a finer scale the findings presented here indicate that although the same ordering can be seen that we see on a broader level, the fine detail shows that inputs and outputs do not simply follow the reversed order seen in broad scale studies (Bedwell et al, 2014, 2015, 2017), but they are in some places more similar to one another in their ordering, showing a greater degree of alignment on this finer scale. This is particularly clear in the dorsal-ventral and anterior-posterior axes (Fig. 4.i. & ii.).

As with comparisons between large and fine scale injections, we revealed further evidence in support of a broad topographic ordering of PFC connections to temporal cortex with the use of tracer injections made into areas of temporal cortex. Consistent with findings from PFC tracer injections, dual injections of Fluoro-Ruby and Fluoro-Gold made into temporal cortex revealed differential ordering of inputs and outputs in the temporal – prefrontal cortex pathway.

Our study of connectivity between PFC and temporal cortices from PRh tracer injections provides evidence to support the fine scale ordering of prefrontal cortex demonstrated by 20-30nl injections. The consistency in our findings from examining the same pathway in both directions indicates the reproducibility of our observed pattern of connectivity.

*Implications for physiological mapping within Prefrontal cortex*

The present study provides evidence that prefrontal connections display a detailed and complex order. An obvious likely consequence for this is that rat prefrontal cortex has the capability to represent mapped information with a relatively detailed resolution. Presently there are not studies to support this idea in rats but there are a few studies which have reported detailed mapping of frontal cortex responses in primates (Sawaguchi & Iba, 2001; Hagler & Sereno, 2006; Hagler et al, 2007; Kastner et al, 2007). Therefore it is possible that physiological mapping supporting cognitive functions (such as memory or attention) could be supported by rodent orbital prefrontal cortex.

*Alignment of connections within the prefrontal-temporal and prefrontal-sensory-motor cortex pathways*

In previous studies we found evidence for non-reciprocal organization in connections from PFC to temporal and sensory-motor cortices. In fact, some injection sites were the same as the present study yet differed in the injection volume and spacing between injections. In the previous studies (Bedwell et al, 2014, 2015) we found differential ordering of input and output connections indicating non-alignment. Specifically, our previous studies identified clear differences in the degree of alignment of connections from dorsal (PL) PFC when compared to more lateral cytoarchitectural PFC regions (VO/VLO, VLO/LO, LO/DLO). For the present study we were able to analyse the ordering at a fine scale, but also at a broader scale by averaging projection locations from adjacent injection sites. The average locations (broad scale) also displayed a differential ordering of input and output connections

in the same region as the previous study. The fine scale locations displayed a different, but not reversed ordering, as was apparent with larger scale injections. Both the average locations and fine scale locations revealed an ordering of inputs and outputs that were not reciprocal. It is noteworthy that in previous studies (Bedwell et al, 2015) the connections between prelimbic cortex and temporal cortex when viewed on a broad scale appeared to be largely reciprocal. The results presented here show that on a smaller scale there is evidence of non-reciprocal connectivity from PL and IL similar to that seen in orbital PFC regions.

*The non-reciprocal organisation of prefrontal input and output connections*

These findings are consistent with our previous studies of prefrontal connectivity, providing evidence of non-reciprocal organization of prefrontal cortex inputs and outputs. The present findings also indicate that this occurs at a broad and fine scale of anatomical connections.

The ordered connections between PFC and temporal and sensory-motor cortices identified here are consistent with evidence of topologically ordered PFC connections from previous studies (Hoover & Vertes, 2011; Kondo & Witter, 2014; Conde et al, 1995; Sesack, 1989). The findings also show evidence of reciprocal connectivity in both PFC pathways studied, consistent with that described in earlier studies (Bedwell et al, 2014, 2015, 2017). In addition to confirming the differential ordering of input and output connections in two PFC pathways, this fine scale analysis also revealed previously undescribed structural properties of connections between PFC and temporal and sensory-motor cortex which could not be observed on a larger scale.

To set these results in context it is important to consider how the current results findings relate to what is known about connectivity of other regions of the cerebral cortex. The primary visual cortex (V1) is a good comparison because so many studies have been made of its structure, organization and

connectivity in mammalian species. In mammals primary visual cortex contains a visual field map which relies on topographically organized feed-forward inputs from the lateral geniculate nucleus (LGN). It also receives topographically organised feedback input connections from areas such as secondary visual cortex (V2) (Sousa et al, 1991) and the middle temporal area (MT) Ungerleider & Desimone, 1986). In return V1 output connections to areas such as V2 (Van Essen et al, 1986), V3 (Lyon & Kaas, 2001) and MT (Rosa et al, 1993) are also topographically organised and reflect the retinotopic input required for the retinotopy present in these regions. Influential hypotheses concerning mechanisms of visual attention (Tootell et al, 1998; Brefczynski & De Yoe, 1999)and feedback (Wang et al, 2006) at least partly depend upon the assumption that visual areas have cortical inputs and outputs that are aligned, therefore making the physical feed-forward and feed-back connections between corresponding regions of visual space in the different visual areas. It would be reasonable to propose that V1 inputs and outputs are not only organized but also aligned (Triplett et al, 2009). Therefore, the evidence concerning detailed reciprocity between visual cortices, coupled with detailed non-reciprocity in PFC connections, implies that visual cortex has a different connectional organization to PFC.

*What is the connectional architecture of Prefrontal cortex?*

*Temporal Cortex*

Further analysis of the relationship between input and output connections in the PFC – temporal cortex pathway revealed by the connectivity matrix (fig. 12) identified otherwise unseen structural properties. The significance of this is that segregated parts of the temporal to prefrontal cortex circuit show feedback from widespread regions of prefrontal cortex. This estimate of prefrontal cortex architecture is likely to be a conservative estimate of the number of feedback connections (from PFC to temporal cortex) because the matrix is based on the strongest labelling of the tracers. It is almost certain that this architectural organisation has a crucial bearing on how this prefrontal-temporal cortex circuitry supports cognitive processing.

*Sensory-motor cortex*

When examining the connectivity matrix (fig. 14) produced for the PFC – sensory-motor cortex pathway, evidence for largely non-reciprocal and widespread connectivity similar to that seen in the temporal cortex pathway can be seen, as well as PFC regions with relatively few return projections. Interestingly, these differences in feedback seem to coincide with the anterior-posterior location of connections in sensory-motor cortex: injection sites receiving more widespread feedback (B [PL], D [VO/VLO] and F [LO/DLO]) produce labelling in more posterior areas of sensory-motor cortex. As with temporal cortex connections, labelling here shows evidence of a high degree of reciprocity as well as non-reciprocal connections in PL.

Notably, the PFC region with a considerably smaller distance between connections (fig. 15), is the same area (VO) that in previous studies has shown evidence of direct connections from primary cortical regions (M1, S1) to PFC (Bedwell et al, 2014 & 2017). This is inconsistent with traditional hierarchical organisation of primary → secondary → association cortical regions → PFC (Fuster, 2001; Botvinick, 2008), which implies connections must be organised from M1 → M2 → association areas → PFC. This may be an indication of the underlying structure of differential functional circuits. Similar to the organisation seen in temporal cortex, we can see that some regions of sensory-motor cortex send and receive some highly reciprocal PFC connections but also non-reciprocal PFC connections in this pathway, indicating a similar non-parallel organisation of this network.

*Conclusion*

This study indicates that the prefrontal to temporal cortex and prefrontal to sensory-motor cortex pathways in the rat consist of detailed topographic maps of afferent and efferent connections. In addition, these connections are not reciprocal at a fine scale (i.e. occur in different cortical locations). This study provides further evidence to confirm previous findings of ordered arrangements of input

and output connections between PFC and two distinct cortical regions, as well as differential ordering and reciprocity of input and output connections. These findings have identified distinct organisational patterns within PFC connections, a structural property that has not previously been described in these pathways.

Reciprocity of cortical connections is a recurring characteristic throughout the brain, said to be hallmark feature of physiological and anatomical organisation, described throughout the cerebral cortex (Wang et al, 2006; Cantone et al, 2005; Agster & Burwell, 2009; Nascimento-Silva et al, 2014). Based on this, the high degree of non-reciprocal connections found in PFC pathways is a surprising observation. However, Haber (2003), described non-reciprocal connections between regions associated with different basal-ganglia circuits. Haber stated that within primate basal ganglia networks there are both reciprocal and non-reciprocal connections between regions with similar functions, many of which involve PFC. This may be a recruiting property throughout the cortex; Haber (2003) concluded that similarly functioning regions are connected by reciprocal connections and regions with greatly differing functions are connected with non-reciprocal connections. Similar observations of reciprocal connectivity have been made elsewhere, often between areas holding similar functions e.g. S1 & S2 (Henry & Catania, 2006; Aronoff et al, 2010) and M1 & S1 (Porter & White, 19983; Aronoff et al, 2010). Observations of more highly topographic and clustered connections from areas of the same functional type in comparison to connections between areas belonging to different functional groups have been observed in auditory cortex in the cat (Lee & Winer, 2008). Based on this knowledge, our findings likely indicate a closer relationship in terms of functional similarity between PL / IL and PRh, ENT and Te, as well as PL with M2 and Cg1, than the comparative relationship between VO, VLO, LO and DLO with the same temporal and sensory-motor regions.

Previous studies have identified distinct functions in orbital PFC regions (Schoenbaum & Esber, 2010; Schoenbaum & Roesch, 2005) compared to mPFC (Vertes, 2006; Narayanan & Laubach, 2006; Kim et al, 2013), providing additional evidence to support differential connectivity. This could mean a difference in levels of complexity or abstraction between the two types of connectivity we have revealed. Further physiological studies are required to determine if these ordered prefrontal connections support physiological maps and organisation of function.

References

Agster, K. L., and Burwell, R. D. (2009). Cortical efferents of the perirhinal, postrhinal, and entorhinal cortices of the rat. Hippocampus, 19(12), 1159-1186.

Arnault, P. & Roger, M. (1990) Ventral temporal cortex in the rat: Connections of secondary auditory areas Te2 and Te3. J Comp Neurol. 302:110-123.

Aronoff, R., Matyas, F., Mateo, C., Ciron, C., Schneider, B. & Petersen, C.C. (2010) Long-range connectivity of mouse primary somatosensory barrel cortex. Eur J Neurosci. 31:2221-2233.

Bayer, S. A., and J. Altman. (1991). Development of the endopiriform nucleus and the claustrum in the rat brain. Neuroscience, 45, 391-412.

Bedwell, S.A., Billett, E.E., Crofts, J.J., Tinsley, C.J. (2014). The topology of connections between rat

prefrontal, motor and sensory cortices. Front Syst Neurosci. 8:177.

Bedwell, S.A., Billett, E.E., Crofts, J.J., MacDonald, D.M. & Tinsley, C.J. (2015). The topology of connections between rat prefrontal and temporal cortices.Front Syst Neurosci. 9:80.

Bedwell, S.A., Billett, E.E., Crofts, J.J. & Tinsley, C.J. (2017). Differences in Anatomical Connections across Distinct Areas in the Rodent Prefrontal Cortex. European Journal of Neuroscience. 45 (6). 859-873.

Berendse, H. W., Galis-de Graaf, Y. & Groenewegen, H. J. (1992). Topographical organization and relationship with ventral striatal compartments of prefrontal corticostriatal projections in the rat. J. Comp. Neurol. 316, 314-347.

Botvinick, M. M. (2008). Hierarchical models of behavior and prefrontal function.

Trends Cogn. Sci. 12, 201–208.

Brefczynski, J. A. & De Yoe, E. A (1999). A physiological correlate of the 'spotlight' of attention. Nat Neurosci. 2, 370-374.

Burwell, R.D., Witter, M.P., & Amaral, D.G. (1995). Perirhinal and postrhinal cortices of the rat: A review of the neuroanatomical literature and comparison with findings from the monkey brain. Hippocampus. 5:390-408.

Canto, C. B., Wouterlood, F. G., and Witter, M. P. (2008). What does the anatomical organization of the entorhinal cortex tell us? Neural Plasticity, 2008, 381243.

Cantone, G., Xiao, J., McFarlane, N. & Levitt, J. B. (2005). Feedback connections to ferret striate cortex: direct evidence for visuotopic convergence of feedback inputs. J. Comp. Neurol. 487, 312-331.

Cavada, C. & Goldman-Rakic, P. S. (1989). Posterior parietal cortex in rhesus monkey: I. Parcellation of areas based on distinctive limbic and sensory corticocortical connections. J Comp Neurol 287, 393-421.

Cavada, C. & Goldman-Rakic, P. S. (1989). Posterior parietal cortex in rhesus monkey: II. Evidence for segregated corticocortical networks linking sensory and limbic areas with the frontal lobe. The Journal of comparative neurology 287, 422-45.

Conde, F., Maire-Lepoivre, E., Audinat, E. & Crepel, F. (1995). Afferent connections of the medial frontal cortex of the rat. II. Cortical and subcortical afferents. J Comp Neurol. 352 (4) 567 – 593.

Delatour, B. & Witter, M.P. (2002). Projections from the parahippocampal region to the prefrontal cortex in the rat: Evidence of multiple pathways. Eur J Neurosci (France) 15:1400-1407.

Fuster, J. M. (2001). The prefrontal cortex—an update: time is of the essence.

Neuron 30, 319–333.

Giguere, M. & Goldman-Rakic, P. S. (1988). Mediodorsal nucleus: areal, laminar, and tangential distribution of afferents and efferents in the frontal lobe of rhesus monkeys. J Comp Neurol 277, 195-213.

Haber, S.N. (2003). The primate basal ganglia: parallel and integrative networks. Journal of chemical neuroanatomy 26, 317-330.

Hagler, D. J.,Jr & Sereno, M. I. (2006). Spatial maps in frontal and prefrontal cortex. Neuroimage 29, 567-577.

Hagler, D. J.,Jr, Riecke, L. & Sereno, (2007). M. I. Parietal and superior frontal visuospatial maps activated by pointing and saccades. Neuroimage 35, 1562-1577.

Henry, E.C. & Catania, K.C. (2006). Cortical, callosal, and thalamic connections from primary somatosensory cortex in the naked mole-rat (heterocephalus glaber), with special emphasis on the connectivity of the incisor representation. Anat Rec A Discov Mol Cell Evol Biol. 288:626-645.

Hoover, W. B. & Vertes, R. P. (2011). Projections of the medial orbital and ventral orbital cortex in the rat. J. Comp. Neurol. 519, 3766-3801.

Kastner, S. et al. (2007). Topographic maps in human frontal cortex revealed in memory-guided saccade and spatial working-memory tasks. Journal of neurophysiology 97, 3494-507.

Kim, J., Ghim, J.W., Lee, J.H. & Jung, M.W. (2013). Neural correlates of interval timing in rodent prefrontal cortex. J Neurosci (United States) 33:13834-13847.

Kondo, H. & Witter, M. P. Topographic organization of orbitofrontal projections to the parahippocampal region in rats. J. Comp. Neurol. 522, 772-793 (2014).

Lee, C. C. and Winer, J. A. (2008), Connections of cat auditory cortex: I. Thalamocortical system. J. Comp. Neurol., 507, 1879–1900.

Lyon, D. C. & Kaas, J. H. (2001). Connectional and architectonic evidence for dorsal and ventral V3, and dorsomedial area in marmoset monkeys. J. Neurosci. 21, 249-261.

Miller, M. W., and Vogt, B. A. (1984). Direct connections of rat visual cortex with sensory, motor, and association cortices. J. Comp. Neurol. 226, 184–202.

Nascimento-Silva, S., Pinon, C., Soares, J. G., and Gattass, R. (2014). Feedforward and feedback connections and their relation to the CytOx modules of V2 in cebus monkeys. The Journal of Comparative Neurology.

Narayanan, N.S. & Laubach, M. (2009). Delay activity in rodent frontal cortex during a simple reaction time task. J Neurophysiol. 101:2859-2871.

Narayanan, N.S. & Laubach, M. (2008). Neuronal correlates of post-error slowing in the rat dorsomedial prefrontal cortex. J Neurophysiol. 100:520-525.

Narayanan, N.S. & Laubach, M. (2006). Top-down control of motor cortex ensembles by dorsomedial prefrontal cortex. Neuron. 52:921-931.

Olson, C.R. & Musil, S.Y. (1992). Topographic organization of cortical and subcortical projections to posterior cingulate cortex in the cat: Evidence for somatic, ocular, and complex subregions. The Journal of Comparative Neurology 324:237-60.

Ongur, D., and Price, J. L. (2000). The organization of networks within the orbital and medial prefrontal cortex of rats, monkeys and humans. Cerebral Cortex (New York, N.Y.: 1991), 10(3), 206-219.

Paxinos G, Watson C (1998) The rat brain in stereotaxic coordinates. San Diego, CA: Academic Press.

Perkel, D. J., Bullier, J. & Kennedy, H. (1986). Topography of the afferent connectivity of area 17 in the macaque monkey: a double-labelling study. The Journal of comparative neurology 253, 374-402.

Porter, L.L. & White, E.L. (1983). Afferent and efferent pathways of the vibrissal region of primary motor cortex in the mouse. J Comp Neurol. 214:279-289.

Reep, R.L., Corwin, J.V. & King, V. (1996) Neuronal connections of orbital cortex in rats: Topography of cortical and thalamic afferents. Exp Brain Res. 111:215-232.

Rosa, M. G., Soares, J. G., M., F.,Jr & Gattass, R. (1993). Cortical afferents of visual area MT in the Cebus monkey: possible homologies between New and Old World monkeys. Visual neuroscience 10, 827-55.

Rose, J. E., and Woolsey, C. N. (1948). The orbitofrontal cortex and its connections with the mediodorsal nucleus in rabbit, sheep and cat. Research Publications - Association for Research in Nervous and Mental Disease, 27, 210-232.

Saleem, K.S., Miller, B and Price, J.L. (2014). Subdivisions and connectional networks of the lateral prefrontal cortex in the macaque monkey. Journal of comparative neurology, 522 (7), 1641-1690.

Sawaguchi, T. and Iba, M. (2001). Prefrontal cortical representation of visuospatial working memory in monkeys examined by local inactivation with muscimol. Journal of neurophysiology 86, 2041-53.

Schilman, E. A., Uylings, H. B., Galis-de Graaf, Y., Joel, D., and Groenewegen, H. J. (2008). The orbital cortex in rats topographically projects to central parts of the caudate-putamen complex. Neuroscience Letters, 432(1), 40-45.

Sesack, S. R., Deutch, A. Y., Roth, R. H. & Bunney, B. S. (1989). Topographical organization of the efferent projections of the medial prefrontal cortex in the rat: an anterograde tract-tracing study with Phaseolus vulgaris leucoagglutinin. J. Comp. Neurol. 290, 213-242.

Schoenbaum, G. & Esber, G.R. (2010). How do you (estimate you will) like them apples? integration as a defining trait of orbitofrontal function. Curr Opin Neurobiol. 20:205-211.

Schoenbaum, G. & Roesch, M. (2005). Orbitofrontal cortex, associative learning, and expectancies. Neuron. 47:633-636.

Smith, N.J., Horst, N.K., Liu, B., Caetano, M.S. & Laubach, M. (2010). Reversible inactivation of rat premotor cortex impairs temporal preparation, but not inhibitory control, during simple reaction-time performance. Front Integr Neurosci. 4:124.

Sousa, A. P., Pinon, M. C., Gattass, R. & Rosa, M. G. (1991). Topographic organization of cortical input to striate cortex in the Cebus monkey: a fluorescent tracer study. The Journal of comparative neurology 308, 665-82.

Stalnaker, T.A., Cooch, N.K. & Schoenbaum, G. (2015) What the orbitofrontal cortex does not do. Nat Neurosci. 18:620-627.

Tootell, R. B. et al. (1998). The retinotopy of visual spatial attention. Neuron 21, 1409-22.

Triplett, J. W et al. (2009). Retinal input instructs alignment of visual topographic maps. Cell 139, 175-185.

Ungerleider, L. G. & Desimone, R. (1986). Cortical connections of visual area MT in the macaque. The Journal of comparative neurology 248, 190-222.

Uylings, H. B., Groenewegen, H. J., and Kolb, B. (2003). Do rats have a prefrontal cortex? Behavioural Brain Research, 146(1-2), 3-17.

Van Essen, D. C., Newsome, W. T., Maunsell, J. H. & Bixby, J. L. (1986). The projections from striate cortex (V1) to areas V2 and V3 in the macaque monkey: asymmetries, areal boundaries, and patchy connections. J. Comp. Neurol. 244, 451-480.

Van De Werd, H. J., and Uylings, H. B. (2008). The rat orbital and agranular insular prefrontal cortical areas: a cytoarchitectonic and chemoarchitectonic study. Brain Struct. Funct. 212, 387–401.

Vertes, R. P. (2004). Differential projections of the infralimbic and prelimbic cortex in the rat. Synapse, 51, 32–58.

Vertes, R. P. (2006). Interactions among the medial prefrontal cortex, hippocampus and

midline thalamus in emotional and cognitive processing in the rat. Neuroscience, 142(1), 1-20.

Wang, W., Jones, H. E., Andolina, I. M., Salt, T. E. & Sillito, A. M. (2006). Functional alignment of feedback effects from visual cortex to thalamus. Nat. Neurosci. 9, 1330-1336.

Figure legends

Figure 1. (i) Coronal section of PFC (AP 4.2mm from Bregma) showing the cytoarchitectural boundaries of the prelimbic (PL), infralimbic (IL), medial orbital (MO), ventral orbital (VO), ventolateral orbital (VLO), lateral orbital (LO) and dorsolateral orbital (DLO) cortices (according to Van de Werd & Uylings, 2008. Dorsal boundary of PL according to Paxinos & Watson, 1998), depicting almagamated sites of Fluoro-Gold and Fluoro-Ruby injections; Prelimbic: A & B, Infralimbic/Medial orbital: C, Ventral orbital/Ventrolateral orbital: D, Ventrolateral orbital/Lateral orbital: E, Lateral orbital/Dorsolateral orbital: F and Dorsolateral orbital: G, with 0.5mm spread. (ii) Coronal section of PFC showing location and spread of (20nl) Fluoro-Ruby at injection site in VLO/LO (R11). (iii) Coronal section of PFC showing location and spread of (30nl) Fluoro-Gold at injection site in PL (R21). (iv) Representations of Fluoro-Ruby (20nl) (R13, R17, R16, R15, R11, R12, R8 (broken line)) injection sites in PL (R13, R17), IL/MO (R16), VO/VLO (R15), VLO/LO (R11), LO/DLO (R12) and DLO (R8) in the right hemisphere. (v) Representations of Fluoro-Gold (30nl) (R13, R21, R19, R20, R16, R12, R9 (solid line)) injection sites in PL (R13, R21), IL/MO (R19) VO/VLO (R20), VLO/LO (R16), LO/DLO (R12) and DLO (R9) in the left hemisphere. Fluoro-Ruby injection sites were predominantly within the boundaries of Fluoro-Gold injection sites. There is some overlap between retrograde injection sites into PL, IL and VO (R13 & R21, R21 & R19, R21 & R20). There is minimal overlap between anterograde injection sites into DLO (R8 & R12). Scale bars = 100μm.

Figure 2. (i) Coronal section showing retrogradely labelled cells (blue) in temporal cortex produced by injection of Fluoro-Gold (30nl) into PL (injection site B: R21). (ii) Coronal section showing retrogradely labelled cells (blue) in temporal cortex produced by injection of Fluoro-Gold (30nl) into DLO (injection site F: R12). (iii) Retrogradely labelled cells in temporal cortex (blue) produced by injection of Fluoro-Gold (30nl) into DLO (injection site F: R12). (iv) Coronal section showing anterogradely labelled axon terminals (red) in temporal cortex produced by injection of Fluoro-Ruby (20nl) into PL (injection site B: R17). (v) Coronal section showing anterogradely labelled axon terminals (red) in temporal cortex produced by injection of Fluoro-Ruby (20nl) into DLO (injection site G: R8). (vi) Anterogradely labelled axon terminals (red) in temporal cortex produced by injection of Fluoro-Ruby (20nl) into IL/MO (injection site C: R16). Arrows denote the location of the rhinal sulcus. Scales bars = 100μm.

Figure 3. Diagram representing the amalgamated injection sites of Fluoro-Gold and Fluoro-Ruby, and the projection sites to temporal cortex for both retrograde (Fluoro-Gold) and anterograde (Fluoro-Ruby) tracer injections. (i) The locations of injection sites A (PL: R13), B (PL: R17, R21), C (IL/MO: R16, R19), D (VO/VLO: R15, R20), E (VLO/LO: R11, R16), F( LO/DLO: R12) and G (DLO: R8, R9) and the location of labelling in temporal cortex. (ii) The locations of retrogradely labelled cells in temporal cortex, resultant from 30nl Fluoro-Gold injections into PFC injection sites A-G (R13, R21, R19, R20, R16, R12, R9). (iii) The locations of anterogradely labelled axon terminals in temporal cortex resultant from 20nl Fluoro-Ruby injections into PFC injection sites A-D (R13, R17, R16, R15, R11, R12, R8).

Figure 4. The mean effect of PFC injection site on the (i) dorsal-ventral, (ii) anterior-posterior and (iii) medial-lateral location of retrogradely labeled cells (n=1122 arising from 7 rats: A(PL:R13)=59, B(PL:R21)=184, C(IL/MO:R19)=360, D(VO/VLO:R20)=92, E(VLO/LO:R16)=39, F(LO/DLO:R12)=194, G(DLO:R9)=194) and anterogradely labeled axon terminals (n=167 arising

from 7 rats: A(PL:R13)=27, B(PL:R17)=24, C(IL/MO:R16)=19, D(VO/VLO:R15)=21, E(VLO/LO:R11)=45, F(LO/DLO:R12)=19, G(DLO:R8)=12) within temporal cortex. Scatterplots represent all raw data points. Horizontal bars indicate mean location of labelling. (iv) Coronal cross section of PFC showing the position of 7 injection sites; PL (A, B), IL/MO (C), VO/VLO (D), VLO/LO (E), LO/DLO (F) and DLO (G). Coronal cross section of temporal cortex showing the three dimensions in which the locations of labels were recorded.

Figure 5. (i) Coronal section showing retrogradely labelled cells (blue) in sensory-motor cortex produced by injection of Fluoro-Gold (30nl) into VO/VLO (D: R20). (ii) Coronal section showing retrogradely labelled cells (blue) in sensory-motor cortex produced by injection of Fluoro-Gold (30nl) into PL (B: R21). Arrow denotes location of retrogradely labeled cells. (iii) Retrogradely labelled cells in sensory-motor cortex (blue) produced by injection of Fluoro-Gold (30nl) into LO/DLO (F: R12). (iv) Coronal section showing anterogradely labelled axon terminals (red) in sensory-motor cortex produced by injection of Fluoro-Ruby (20nl) into PL (B: R17). (v) Anterograde labelling (red) in sensory-motor cortex produced by injection of Fluoro-Ruby (20nl) into DLO (G: R8). (vi) Anterograde labelling (red) in temporal cortex produced by injection of Fluoro-Ruby (20nl) into VLO/LO (E: R11). Scales bars = 100μm.

Figure 6. Diagram representing the almagamated injection sites of Fluoro-Gold and Fluoro-Ruby, and the projection sites to sensory-motor cortex for both retrograde (Fluoro-Gold) and anterograde (Fluoro-Ruby) tracer injections. (i) The locations of injection sites A (PL: R13), B (PL: R17, R21), C (IL/MO: R16, R19), D (VO/VLO: R15, R20), E (VLO/LO: R11, R16), F( LO/DLO: R12) and G (DLO: R8, R9). (ii) The locations of retrogradley labelled cells in sensory-motor cortex, resultant from 30nl Fluoro-Gold injections into PFC injection sites A-G (R13, R21, R19, R20, R16, R12, R9). Note the concentration of retrograde labelling in layers V and VI, with laminar ordering present. (iii)

The locations of anterogradely labelled axon terminals in sensory-motor cortex resultant from 20nl Fluoro-Ruby injections into PFC injection sites A-D (R13, R17, R16, R15, R11, R12, R8).

Figure 7. The mean effect of PFC injection site on the (i) dorsal-ventral, (ii) anterior-posterior and (iii) medial-lateral location of retrogradely labeled cells (n= 597 arising from 7 rats: A(PL:R13)=119, B(PL:R21)=52, C(IL/MO:R19)=91, D(VO/VLO:R20)=85, E(VLO/LO:R16)=22, F(LO/DLO:R12)=71, G(DLO:R9)=157) and anterogradely labeled axon terminals (n=305 arising from 7 rats: A(PL:R13)=34, B(PL:R21)=138, C(IL/MO:R19)=63, D(VO/VLO:R20)=24, E(VLO/LO:R16)=22, F(LO/DLO:R12)=10, G(DLO:R9)=14) within sensory-motor cortex. Scatterplots represent all raw data points. Horizontal bars indicate mean location of labelling. (iv) Coronal cross section of PFC showing the position of 7 injection sites; PL (A, B), IL/MO (C), VO/VLO (D), VLO/LO (E), LO/DLO (F) and DLO (G). Coronal cross section of sensory-motor cortex showing the three dimensions in which the locations of labels were recorded.

Figure 8. Three dimensional representations of labelling seen in (i, ii) temporal cortex and (iii, iv) sensory-motor cortex. (i) 3D locations of retrograde labels seen in temporal cortex from PFC injections of Fluoro-Gold. (ii) 3D locations of anterograde labels seen in temporal cortex from PFC injections of Fluoro-Ruby. (iii) 3D locations of retrograde labels seen in sensory-motor cortex from PFC injections of Fluoro-Gold. (iv) 3D locations of anterograde labels seen in sensory-motor cortex from PFC injections of Fluoro-Ruby.

Figure 9. Coronal sections of temporal cortex showing the locations and spread of dual tracer injections (50 nl Fluoro-Gold & 50 nl Fluorescein, R48, R49, R50, R51) and single injection (50 nl Fluoro-Gold, R47), separated by 0.5 mm.

Figure 10. Diagram representing the projection sites to prefrontal cortex for both retrograde (Fluoro-Gold) and anterograde (Fluorescein) injections made into temporal cortex. Coronal sections of PFC showing (i) retrograde (R47, R48, R49, R50, R51) and (ii) anterograde (R48, R49, R50, R51) labelling resultant from dual injections of Fluoro-Gold and Fluorescein into temporal cortex and single injection of Fluoro-Gold (50 nl) into temporal cortex at bregma -2.8mm.

Figure 11. The mean effect of temporal injection site on the (i) dorsal-ventral, (ii) anterior-posterior and (iii) medial-lateral location of retrogradely labeled cells (n= 284) arising from 5 rats: Bregma -2.8, R47 (n=33), -3.3, R45 (n=139), -3.8, R48 (n=9), -4.3, R49 (n=74), -4.8, R50 (n=29) and anterograde labels arising from 4 rats: (n= 448) Bregma -3.3, R51 (n=124), -3.8, R48 (n=74), -4.3, R49 (n=154), -4.8, R50 (n=96) within prefrontal cortex. Scatterplots represent all raw data points. Horizontal bars indicate mean location of labelling. (iv) Coronal cross section of prefrontal cortex showing the three dimensions in which the locations of labels were recorded.

Figure 12. Connectivity matrix showing the relationship between input and output connections from PFC to temporal cortex. X = Retrograde and anterograde labelling found in the same cytoarchitectural regions of temporal cortex. X = Reciprocal connection: Retrograde and anterograde labelling from the same PFC injection site is found in the same cytoarchitectural region of temporal cortex. E.g. Retrograde projection site A (PL) is found in the same cytoarchitectural region as anterograde projections A (PL), B (PL) and E (VLO/LO).

Figure 13. The effect of PFC retrograde (Fluoro-Gold) injection site on the reciprocity index, derived from connectivity matrix (Fig.11): median distance between Fluoro-Gold and Fluoro-Ruby PFC injection sites of retrograde and anterograde labelling found in the same cytoarchitectural regions of temporal cortex. A distance of 1 PFC injection site is given a value of 1 (e.g. the distance between

retrograde site A (dorsal PL) and anterograde site B (ventral PL) = 1). The absolute value is taken, regardless of direction. Regions where no anterograde projections were found in the same cytoarchitectural region as the retrograde connection (e.g. injection site G [DLO]) were not included, as a value of zero here represents an entirely reciprocal connection. Where a retrograde projection is found in the same region as multiple anterograde projections a median distance is calculated. Fluoro-Gold injection sites made into the same PFC sub-regions (i.e. PL) are combined. Injection G (DLO) is excluded due to having no return connections. PL = A & B, MO = C, VO = D, VLO = E, LO = F. Scatterplots represent all raw data points.

Figure 14. Connectivity matrix showing the relationship between input and output connections from PFC to sensory-motor cortex. X = Retrograde and anterograde labelling found in the same cytoarchitectural regions of sensory or motor cortex. X = Reciprocal connection: Retrograde and anterograde labelling from the same PFC injection site is found in the same cytoarchitecural region of sensory or motor cortex. E.g. Retrograde injection site A (PL) receives input connections from a region of sensory-motor cortex which injection site E (VLO/LO) sends output connections to.

Figure 15. The effect of PFC retrograde (Fluoro-Gold) injection site on the median distance between Fluoro-Gold and Fluoro-Ruby PFC injection sites of retrograde and anterograde labelling found in the same cytoarchitectural regions of sensory-motor cortex. A distance of 1 PFC injection site is given a value of 1 (e.g. the distance between retrograde site A [PL] and anterograde site B [PL] = 1). Where a retrograde projection is found in the same region as multiple anterograde projections a median distance is calculated. Fluoro-Gold injection sites made into the same PFC sub-regions (i.e. PL) are combined. PL = A & B, VO= D, LO=F, DLO=G. Injection G (DLO) is excluded due to having no return connections. Error bars = standard error. Scatterplots represent all raw data points.

| Rat ID | Tracer | volume (nl) | AP (mm) | ML (mm) | Depth from cortical surface (mm) | Angle (°) |
|---|---|---|---|---|---|---|
| 8 | Fluoro-Ruby | 20 | 3.7 | 3.2 | 3.2 | 0 |
| 9 | Fluoro-Gold | 30 | 3.7 | 3.2 | 3.2 | 0 |
| 11 | Fluoro-Ruby | 20 | 3.7 | 2.2 | 3.2 | 0 |
| 12 | Fluoro-Gold | 30 | 3.7 | 2.6 | 3.2 | 0 |
| 12 | Fluoro-Ruby | 20 | 3.7 | 2.6 | 3.2 | 0 |
| 13 | Fluoro-Gold | 30 | 3.7 | 1.2 | 2.2 | 0 |
| 13 | Fluoro-Ruby | 20 | 3.7 | 1.2 | 2.2 | 0 |
| 15 | Fluoro-Ruby | 20 | 3.7 | 1.7 | 3.2 | 0 |
| 16 | Fluoro-Gold | 30 | 3.7 | 2.2 | 3.2 | 0 |
| 16 | Fluoro-Ruby | 20 | 3.7 | 1.2 | 3.2 | 0 |
| 17 | Fluoro-Ruby | 20 | 3.7 | 1.2 | 2.7 | 0 |
| 19 | Fluoro-Gold | 30 | 3.7 | 1.2 | 3.2 | 0 |
| 20 | Fluoro-Gold | 30 | 3.7 | 1.7 | 3.2 | 0 |
| 21 | Fluoro-Gold | 30 | 3.7 | 1.2 | 2.7 | 0 |
| 45 | Fluoro-Gold | 50 | -3.3 | 4.5 | 6.7 | 20 |
| 47 | Fluoro-Gold | 50 | -2.8 | 4.5 | 6.7 | 20 |
| 48 | Fluoro-Gold | 50 | -3.8 | 4.8 | 6.7 | 16 |
| 48 | Flourescein | 50 | -3.8 | 4.8 | 6.7 | 16 |
| 49 | Fluoro-Gold | 50 | -4.3 | 4.5 | 6.7 | 16 |
| 49 | Flourescein | 50 | -4.3 | 4.5 | 6.7 | 16 |
| 50 | Fluoro-Gold | 50 | -4.8 | 4.5 | 6.7 | 22 |
| 50 | Flourescein | 50 | -4.8 | 4.5 | 6.7 | 22 |
| 51 | Flourescein | 50 | -3.3 | 4.5 | 6.7 | 20 |
| 51 | Fluoro-Gold | 50 | -3.3 | 4.5 | 6.7 | 20 |

Table 1. Stereotaxic location of tracer injections for each individual rat. Location in terms of anterior-posterior (AP), medial-lateral (ML) and depth from cortical surface (all in mm). These reflect the surgical stereotaxic coordinates rather than histological coordinates).

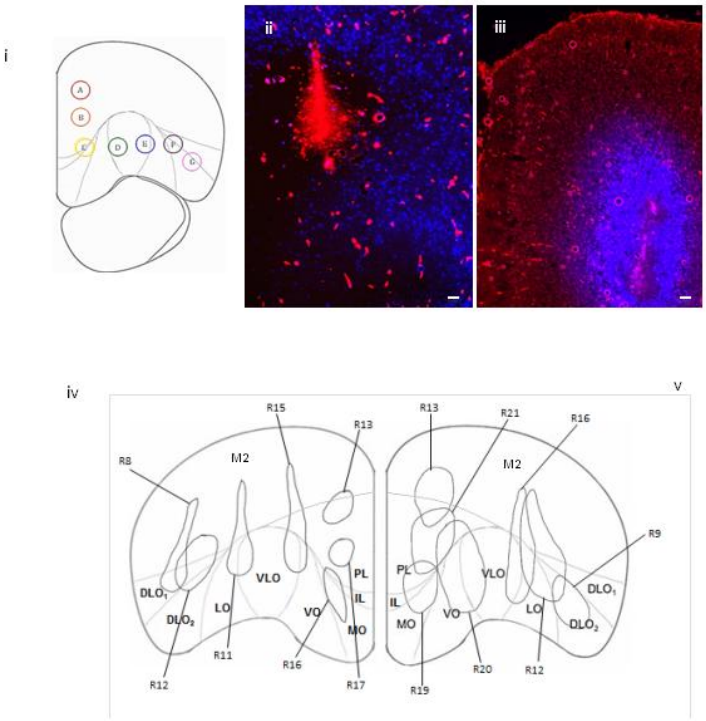

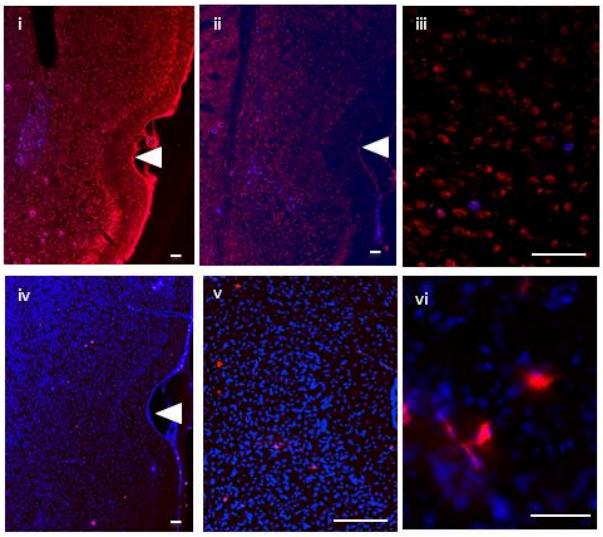

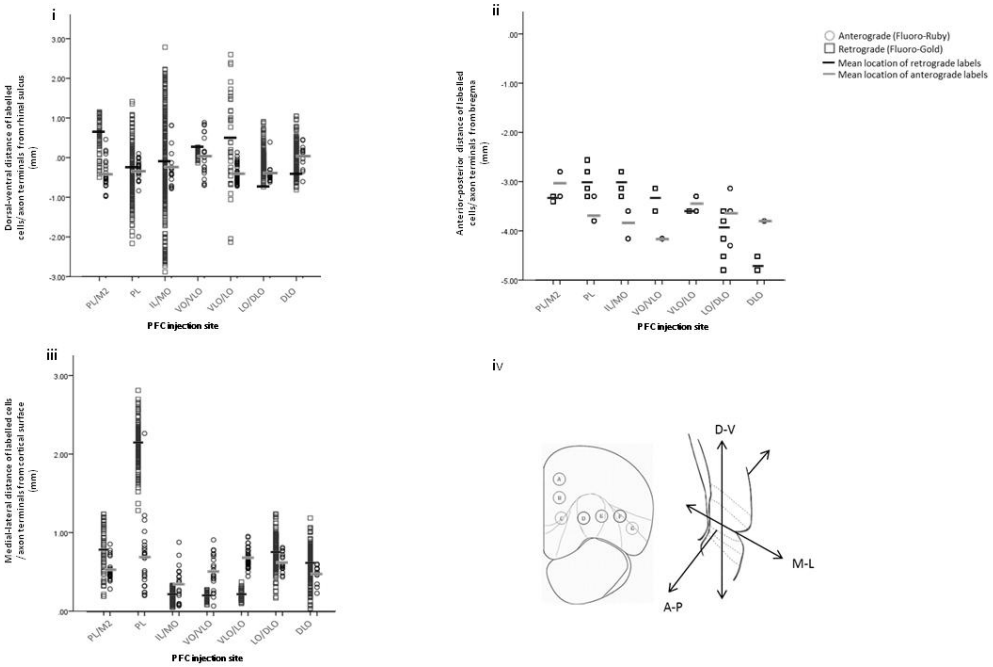


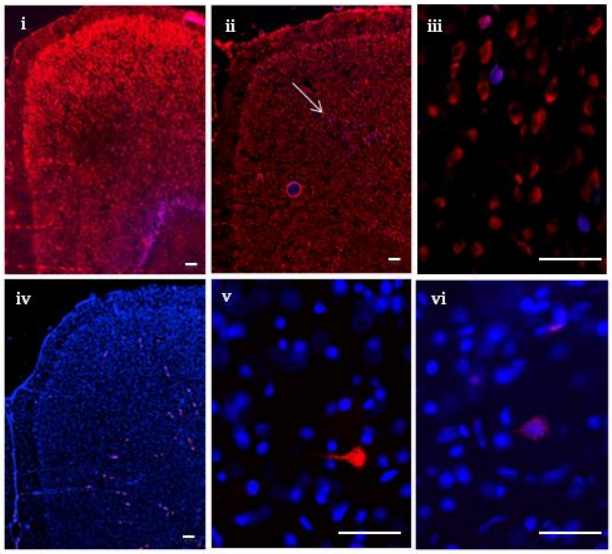

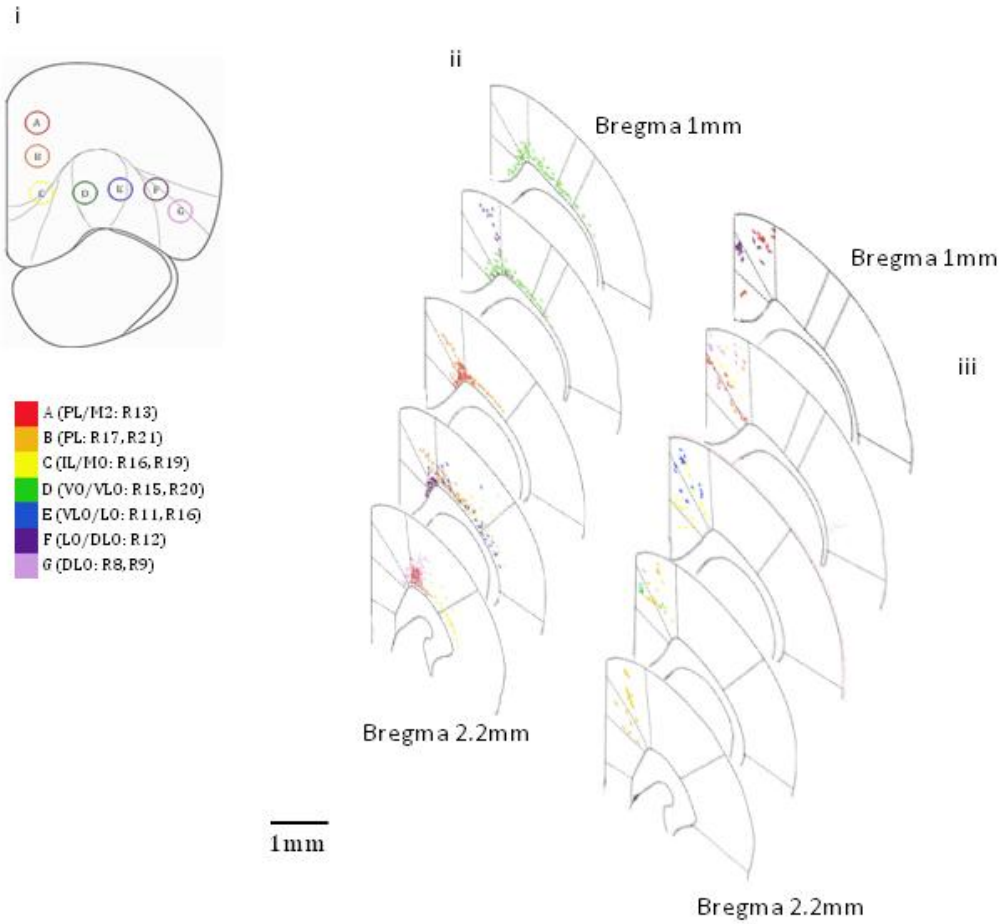

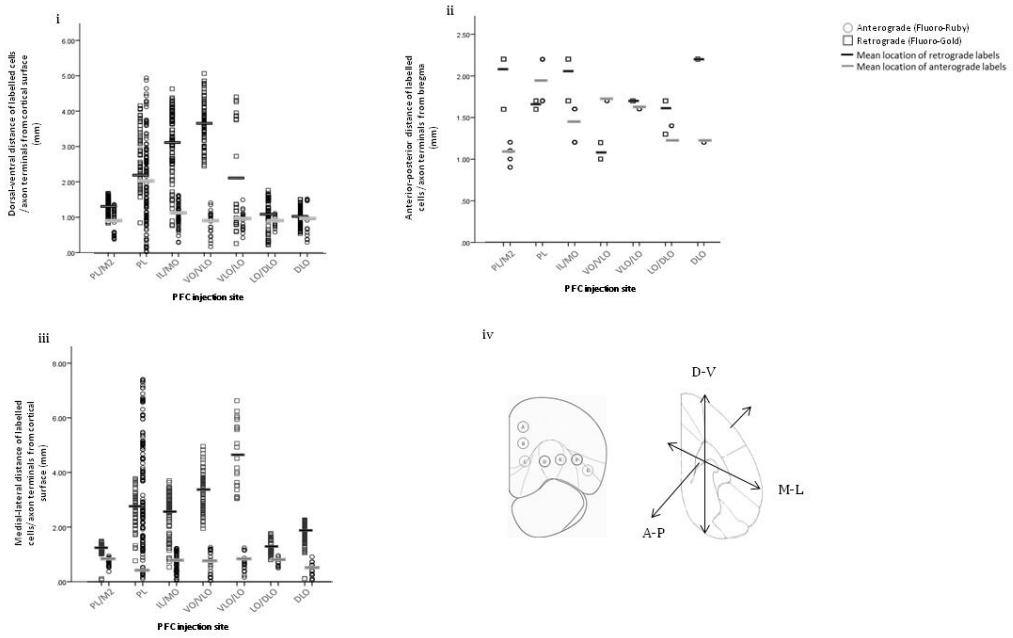


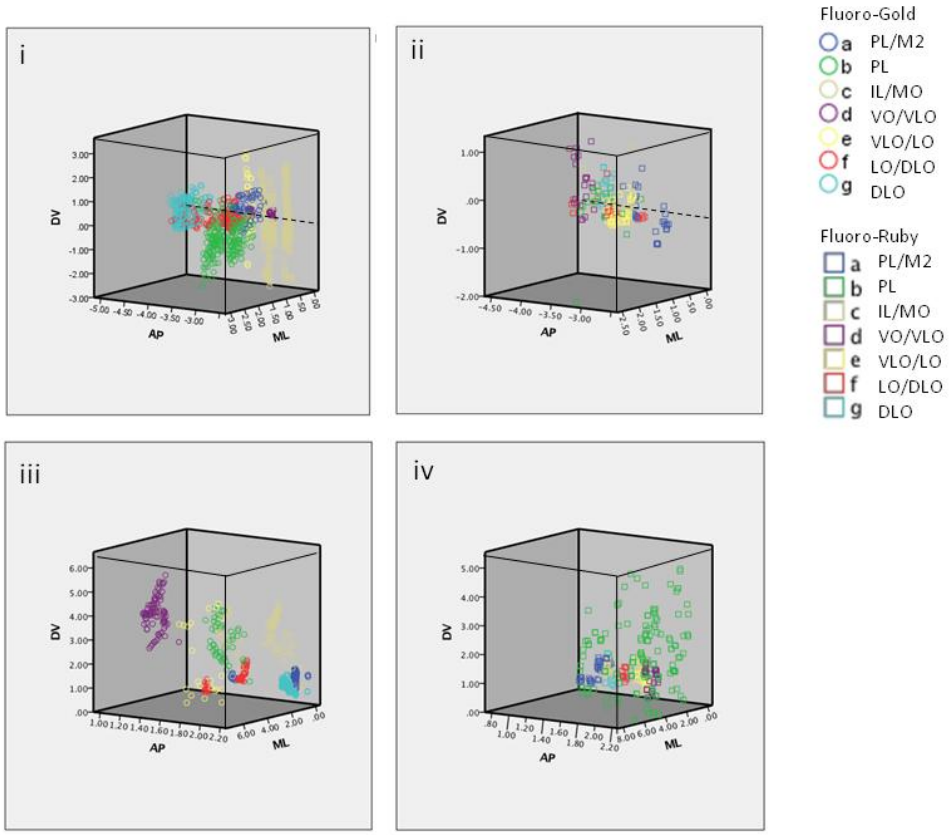

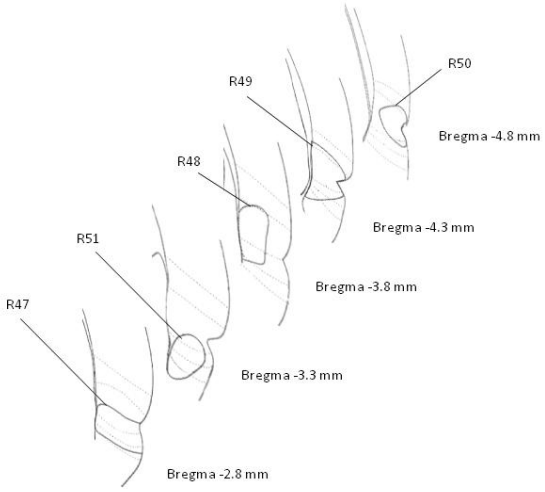


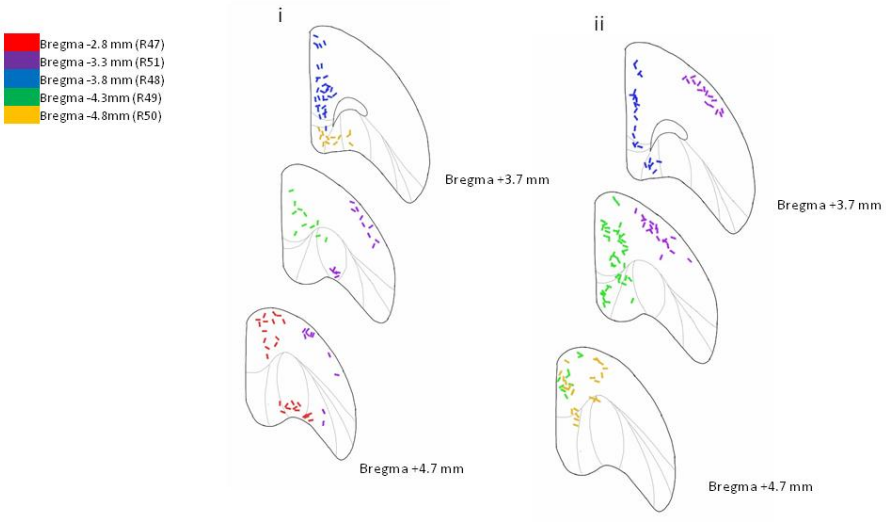

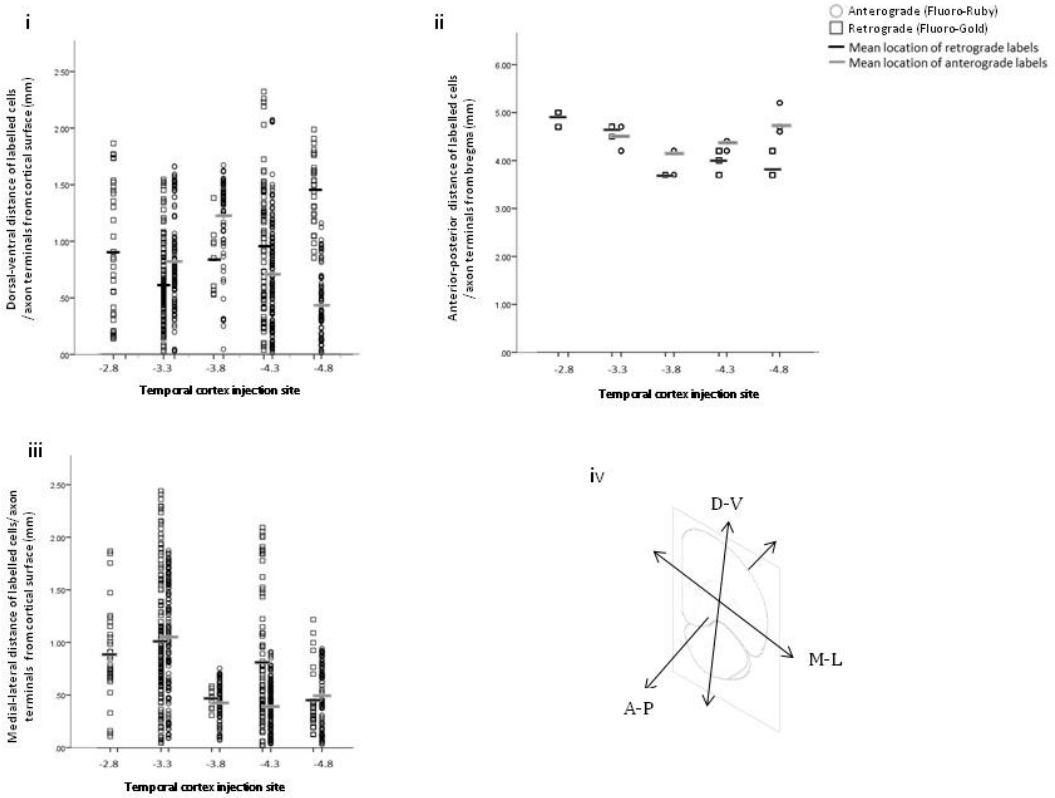

Anterograde projection

| Retrograde projection | PL/ M2 | PL | IL/ MO | VO/ VLO | VLO/ LO | LO/ DLO | DLO |
|---|---|---|---|---|---|---|---|
| PL/M2 | X | X | | | X | | |
| PL | X | X | | | X | X | |
| IL/MO | X | X | | | X | X | |
| VO/VLO | | | | | X | X | |
| VLO/LO | | | | | X | X | |
| LO/DLO | | | X | X | X | X | |
| DLO | | | | | | | |

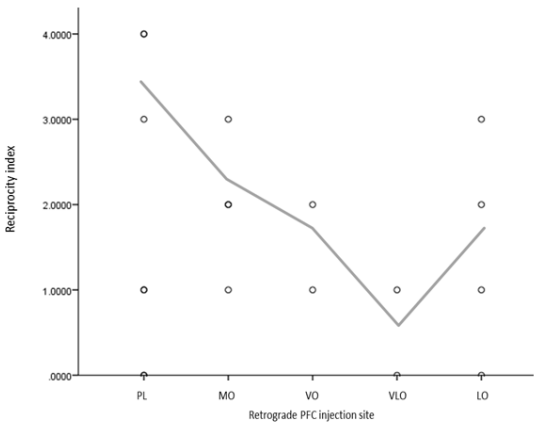

Anterograde projection

| Retrograde projection | PL/ M2 | PL | IL/MO | VO/ VLO | VLO/ LO | LO/ DLO | DLO |
|---|---|---|---|---|---|---|---|
| PL/M2 | | | | | X | | |
| PL | | X | | X | X | | |
| IL/MO | | | | | | | |
| VO/VLO | X | | X | | | X | X |
| VLO/LO | | | | | | | |
| LO/DLO | X | X | X | X | | | X |
| DLO | | X | | | | | |